Environmental Science
Processes & Impacts

RSC Publishing

PAPER

View Article Online
View Journal | View Issue

Open Access Article. Published on 08 October 2013. Downloaded on 6/2/2026 11:35:24 PM.
This article is licensed under a Creative Commons Attribution 3.0 Unported Licence.

Cite this: *Environ. Sci.: Processes Impacts*, 2013, **15**, 2220

Model-based exploration of the drivers of mountain cold-trapping in soil†

John N. Westgate‡ and Frank Wania*

A pollutant is said to undergo mountain cold-trapping if it is found at higher concentrations in a surface medium (soil, snow, foliage) high on a mountain, where it is colder, than in the same medium lower on the mountain. The processes that lead to mountain cold-trapping in soil were explored for a set of hypothetical Perfectly Persistent Pollutants (PPPs) by varying several environmental parameters in a fugacity based fate and transport box model. These parameters were: the spatial scale of the mountain; the rate and location of rain; the amount of particles in the atmosphere; the presence and magnitude of the upslope temperature gradient. The relative potential of each hypothetical PPP to exhibit mountain cold-trapping was expressed in terms of its Mountaintop Contamination Potential (MCP). The PPPs with the highest MCPs were those that neither were deposited from the atmosphere to the surface in the lower zones in the model nor left the model domain without being deposited at all. The simulations revealed that under most conditions wet-gaseous deposition is the biggest driver of mountain cold-trapping in soils, and its effects are greatly enhanced by large negative temperature gradients and increased precipitation upslope. Dry-gaseous and wet-and-dry-particle deposition processes cause similar PPPs to exhibit mountain cold-trapping, and the contributions to MCP by the dry processes are of the same magnitude as wet-particle deposition. Dry gaseous deposition alone is insufficient to cause mountain cold-trapping in soils under any conditions modelled here. Those measuring organic contaminants in mountains should expect to find that mountains with different climates cold-trap different pollutants, and that some mountains may not exhibit upslope enrichment of any species.

Received 19th July 2013
Accepted 8th October 2013

DOI: 10.1039/c3em00385j

rsc.li/process-impacts

Environmental impact

Airborne organic pollutants can become concentrated in surface media in cooler places such as in the high mountains in a process known as cold-trapping. Field studies of the phenomenon have revealed large variations between mountains, both in the extent of cold-trapping and the identity of the pollutants trapped. A computer model is used to explore what processes contribute to mountain cold-trapping of which pollutants, and to explain why some mountains cold-trap certain pollutants and others do not.

Introduction

Persistent Organic Pollutants (POPs) are a set of long-lived chemicals that share several negative characteristics, one of which is the tendency to travel long distances and become concentrated in areas far from their points of release, including Earth's poles.[1] Wania and Mackay[2] proposed that, to a large part, it is the temperature difference between the tropics and the poles that drives this: POPs with volatilities within a certain range can volatilize in the warm tropics or temperate regions but upon arrival in the colder polar regions lack the energy to remain in the atmosphere, either becoming bound to atmospheric particles and being deposited with them or depositing directly to surface media including soils and water. Once there, such contaminants are also less likely to re-volatilize and be transported away than in warmer regions, although decreasing global concentrations can turn the process around.[3] This mechanism, now called polar cold-trapping, can be reinforced by lower rates of degradation in polar regions, which have both lower atmospheric concentrations of hydroxyl radical and lower biological activity than warmer regions. Together these can lead to concentrations of POPs in similar environmental media with similar histories of exposure being higher in polar regions than closer to where the POPs are made and used.[4] For example, pine needles in areas not directly influenced by local inputs of persistent

Department of Chemistry and Department of Physical and Environmental Sciences, University of Toronto Scarborough, 1265 Military Trail, Toronto, Ontario, Canada M1C 1A4. E-mail: frank.wania@utoronto.ca

† Electronic supplementary information (ESI) available. See DOI: 10.1039/c3em00385j

‡ This author can now be contacted at: westgajn@westminster.edu

This journal is © The Royal Society of Chemistry 2013

Open Access Article. Published on 08 October 2013. Downloaded on 6/2/2026 11:35:24 PM.
This article is licensed under a Creative Commons Attribution 3.0 Unported Licence.

pesticides had higher contaminant loads in cooler than warmer regions of Europe, but areas with a history of application contain the bulk of the compounds.[5]

If a temperature difference drives polar cold-trapping, it stands to reason that other environmental temperature gradients, such as those on mountains, will also cause cold-trapping. Indeed, as soon as investigators began to look, evidence was found suggesting hexachlorobenzene (HCB) undergoes mountain cold-trapping, and is found at higher concentrations in plants at high elevations than lower areas at the same latitude.[6] A review of organic contaminants in mountains provides several more examples[7] and workers around the world continue to find evidence of the phenomenon.[8–13]

There are a host of differences between any two environments that could affect the relative concentrations of POPs measured in them. Determining the factors responsible for any observed differences in concentrations of individual POPs is, therefore, a challenge. Computer models allow the simulation of any environment – even an entirely unrealistic one – and the creation of virtual environments that differ in as little as one aspect. Comparing which model inputs lead to important differences in model outputs can give clues about which mechanisms may be responsible for the observations made in real systems. While examinations of polar cold-trapping using models have been ongoing for several years[14,15] mountain cold-trapping has been less frequently explored.[16–18]

A comparison of the identities of the organic contaminants that are found to undergo mountain cold-trapping in the literature reveals that they are modestly different from those found to exhibit polar cold-trapping; for instance, mountains tend to cold-trap less volatile PCB congeners than Earth's Poles do.[18] When compared, model outputs from earlier mountain modelling work in our group[19] and the global scale fate and transport model GloboPOP[15] reflected these differences,[18] but exactly which differences between the two models led to this result have not yet been examined.

Additionally, it is also found that organic contaminants found to exhibit cold-trapping on some mountains are not found to do so on other mountains: for example Kirchner *et al.*[9] found that two hexachlorocyclohexanes, HCB and mirex were found in higher concentrations upslope along only 3 or 4 of 7 elevational transects in the Alps. This may in part be explained by the temperature dependent efficiency with which precipitation scavenging occurs,[18] but mountains differ in more than just the temperature of the precipitation.

Here the fugacity based fate and ransport box model, MountainPOP, was employed to explore which model conditions could lead to the differential cold-trapping of SVOCs observed by researchers. The obvious contrast between the globe and a mountain is the spatial scale. Clear differences between mountains include the magnitude of the temperature gradient from bottom to top, the presence and location of precipitation, and the concentration of atmospheric particles. The changes to the model parameterization that lead to outputs reflecting the actual measurements may hint at the underlying mechanisms.

Methods

Conceptual framework for environmental partitioning in the atmosphere

Where an organic substance resides in the environment depends largely on its relative affinity for the gas phase, aqueous phases and organic phases. The equilibrium partition coefficients of a neutral organic substance between gas phase, water and octanol are commonly used to approximate this relative affinity.[20] These three coefficients are the octanol–air equilibrium partition coefficient (K_{OA}), the water–air equilibrium partition coefficient (K_{WA}), and the octanol–water equilibrium partition coefficient (K_{OW}). Because of the thermodynamic relationship between these three coefficients, two are often sufficient to describe the partitioning characteristics of a neutral organic substance and it is possible to define a two-dimensional partitioning space.[21] The equilibrium distribution of all neutral organic substances between gas phase, water and organic matter can thus be visualized in Chemical Space Plots (CSP).[21] Most environmental media contain multiple phases, *e.g.* the atmosphere comprises not just the gas phase, but also contains organic particulate matter and liquid water. Fig. 1 displays the CSP for the equilibrium phase distribution in the atmosphere (assuming a liquid water content of 10^{-5} and a particle volume fraction of 10^{-11} and a particle organic content of 0.1, giving an organic particle volume fraction of 10^{-12}) for all substances with a $\log_{10} K_{WA}$ from −3 to 10 and a $\log_{10} K_{OA}$ from 3 to 16.[22] Substances with a low K_{WA} and a low K_{OA} – in the upper left portion of the graph – are found almost entirely in the gas-phase, coloured yellow. Similarly, a substance with a high K_{WA} and low to middling K_{OA} will be found primarily in cloud droplets, and one with a high K_{OA} will reside primarily on or in organic particles. The relative sizes of the coloured areas on the graph are in part controlled by the volume of the phase, so that were the particle concentration to increase, the brown area would increase in size relative to the other two phases.[22]

The behaviour of substances with partitioning properties in the transition areas between the yellow, blue and brown fields is of considerable interest. Consider substance *X* with a $\log_{10} K_{WA}$ of 0 and a $\log_{10} K_{OA}$ of 11.5 at 25 °C. At equilibrium, 90% of the mass of substance *X* would be found in the gas phase of this atmosphere, and 10% would be associated with particles, while almost none would be found in the rain droplets. 90% of substance *Y* with a $\log_{10} K_{WA}$ of 0 and a $\log_{10} K_{OA}$ of approximately 13.5 would be found associated with particles, while only 10% would be in the gas phase. With a $\log_{10} K_{OA}$ halfway between the two, a substance would be found in equal masses in both particle and gas phase.

A similar situation applies to a substance *Z* with $\log_{10} K_{OA}$ of 6.5 and $\log_{10} K_{WA}$ of 4, and is primarily found in the gas phase and partly dissolved in rain water at 25 °C. Thus, 90% of the mass of a substance with combinations of equilibrium partition properties that fall on the dark yellow line separating the bright and pale yellow areas would be found in the gas phase in this atmosphere. Similarly, 90% of a substance with properties falling on the dark brown line separating the bright and pale brown areas would be associated with particles and 90% of a

Open Access Article. Published on 08 October 2013. Downloaded on 6/2/2026 11:35:24 PM.
This article is licensed under a Creative Commons Attribution 3.0 Unported Licence.

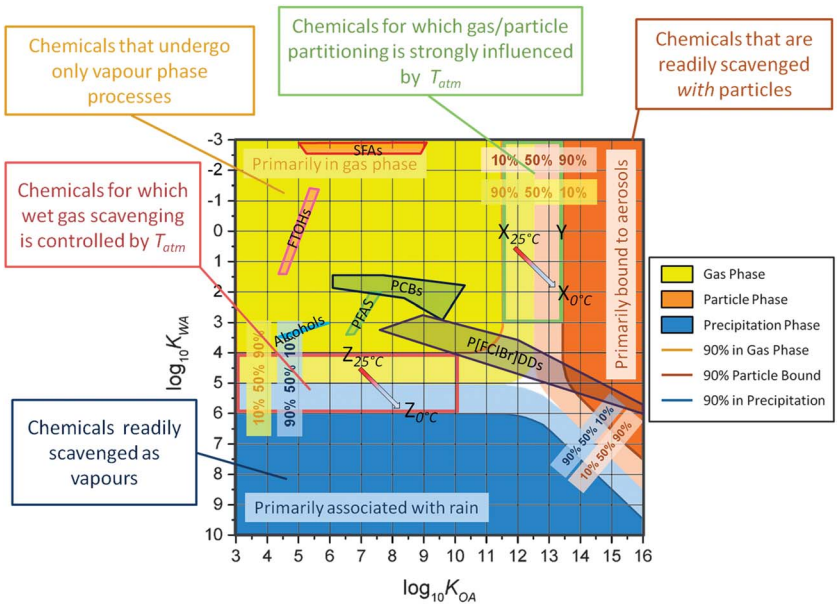

Fig. 1 Equilibrium phase distribution of organic substances in a theoretical atmosphere as a function of their partitioning properties: >90% of the mass of chemicals with a combination of $\log_{10} K_{WA}$ and $\log_{10} K_{OA}$ in the bright yellow area is in the gas phase; >90% of the mass of chemicals in the bright blue area is in rain water; >90% of the mass of each chemical in the bright brown area is associated with particles; 90% of the mass of each chemical with combinations of properties that lie on the dark yellow, dark blue or dark brown lines would reside in the gas, cloud water or particle phase, respectively, while 10% of the masses of each resides in at least one of the other two phases; >50% but <90% of the mass of each chemical with combinations of properties falling within the pale yellow, pale blue or pale brown areas would reside in the gas, cloud water or particle phases, respectively; whether the chemicals in the red box are mostly in the gas-phase or mostly in rain water depends strongly on the temperature of the air (T_{atm}); whether the chemicals in the green box are mostly in the gas-phase or mostly associated with particles depends strongly on T_{atm}; the property combinations of several real families of organic chemicals at 25 °C are plotted: alcohols delineated by the cyan box are non-water-miscible *n*-alcohols,[29] FTOHs delineated by the pink box are fluorotelomer alcohols,[27] PCBs delineated by the navy polyhedron are polychlorinated biphenyls,[30] PFAS delineated by the lime box are perfluoroalkylsulfonamides,[27] P[FClBr]DDs delineated by the purple polyhedron are polyhalogenated dibenzo-*p*-dioxins,[31] and SFAs delineated by the red trapezium are semifluorinated alkanes.[32]

substance with properties falling on the dark blue line separating the bright and pale blue areas would be found dissolved in rain water. Substances with equilibrium partitioning properties between these dark lines are found in significant amounts in more than one phase.

Equilibrium partitioning properties can be very sensitive to temperature,[20] changing by more than 3 orders of magnitude over the range of environmentally relevant temperatures (*ca.* −20 °C to +35 °C). For many substances this will appreciably affect their distribution in the environment. Again consider substance *X*, which was judged above to be 90% in the gas phase. If we assume its partitioning properties K_{WA} and K_{OA} to increase by 2 log units when temperature drops to 0 °C, then the CSP in Fig. 1 suggests that 90% would be associated with particles in the atmosphere. Similarly, substance *Z* undergoes a 2 log unit increase in both K_{OA} and K_{WA} as the temperature drops from 25 °C to 0 °C it moves from being 90% in the gas phase to 90% in the rain water. The red and green boxes in Fig. 1 highlight ranges of equilibrium partitioning properties for substances that would be expected to undergo significant changes in environmental phase distribution in the atmosphere with changes in air temperature (T_{atm}). It makes intuitive sense that at lower temperatures substances tend to move toward the condensed phases of rain water and particles. This partitioning of a substance between air, water and particles determines the processes by which it is removed from the atmosphere.

Atmospheric deposition to surface media

For a substance to be considered cold-trapped on a mountain, it must undergo some process of deposition to surface media from the atmosphere that is driven by temperature. Wet-gaseous deposition is the process in which rain scavenges gas-phase substances and deposits them to surface media such as soil, vegetation or surface waters. Thus, whether a substance is primarily in the gas-phase or dissolved in rain water controls whether or not it is appreciably scavenged by this mechanism. The red box in Fig. 1 highlights the range of partitioning properties of substances for which T_{atm} controls wet-gaseous scavenging. A substance that remains largely in the gas-phase at the temperatures low on the mountain would not be appreciably scavenged by rain and remains in the atmosphere to potentially be advected further up the mountain. If the substance undergoes a significant change in atmospheric phase distribution into the rain water due to the decrease in temperature higher on the mountain, as described above, it may then be subject to wet-gaseous deposition higher in the mountain and become cold-trapped (Fig. 2, middle panel).

Substances associated with particles are subject to deposition from the atmosphere to surfaces either by the particle settling – called dry-particle deposition – or by the particle being washed from the atmosphere by precipitation – called wet-particle deposition. A substance that is not appreciably associated with particles at the temperature at the bottom of the

 This journal is © The Royal Society of Chemistry 2013

Open Access Article. Published on 08 October 2013. Downloaded on 6/2/2026 11:35:24 PM.
This article is licensed under a Creative Commons Attribution 3.0 Unported Licence.

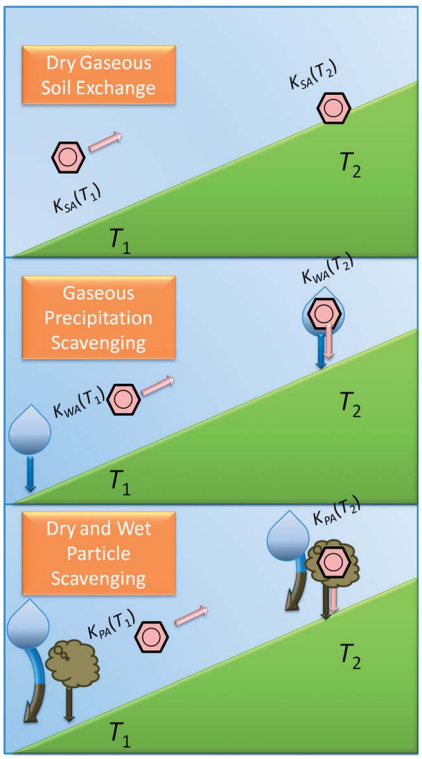

Fig. 2 The processes by which mountain cold-trapping occurs: to become cold-trapped by dry-gaseous deposition a PPP (pink) must have a soil–air equilibrium partition coefficient K_{SA} at the temperature lower on the mountain (T_1) that prevents it from sorbing too much to soil directly from air lower on the mountain and a K_{SA} at the temperature high on the mountain (T_2) that causes it to sorb to soil directly from air so that it does not all exit the system (top); to become cold-trapped by wet-gaseous deposition a PPP must have a water–air equilibrium partition coefficient K_{WA} at T_1 that prevents it from partitioning mostly to precipitation (P↓) and thus be deposited with it and so it is available to move further upslope, and must have a K_{WA} at T_2 so that it partitions from air to P↓ and is deposited to the surface with P↓ there (middle); to become cold-trapped by wet- or dry-particle deposition a PPP must have a particle–air equilibrium partition coefficient K_{PA} at T_1 that prevents it from sorbing to particles and being dry-deposited or P↓ scavenged with the particles so it can proceed upslope and must also have a K_{PA} at T_2 causing it to partition to particles so that is either dry deposited or P↓ scavenged with the particles higher on the mountain (bottom).

mountain remains in the gas phase and can potentially be advected further up the mountain. If the substance is significantly more sorbed to particles at the cooler temperature at the top of the mountain, then that substance can be deposited *via* dry- or wet-particle deposition and is thus cold-trapped (Fig. 2, bottom). Those substances with combinations of partitioning properties in the green box of Fig. 1 are those for which T_{atm} controls whether or not they are subject to particle-bound scavenging, and thus this form of cold-trapping.

The simplest process that moves substances from the atmosphere to the surface is dry-gaseous deposition: a substance that partitions significantly more to the atmospheric gas phase than to the Earth's surface (soil, vegetation, water bodies) at the warm temperature at the bottom of a mountain, but significantly more to the surface than the atmospheric gas phase at the cooler temperature at the top of the mountain would be cold-trapped (Fig. 2, top). The magnitude of this mode of scavenging is limited somewhat by this exchange occurring only at the contact surface between the atmosphere and the surface, while the wet processes and exchange with airborne particles occur throughout the volume of the atmosphere.

The model

MountainPOP2.0 is a fugacity based dynamic (non-steady-state) fate and transport box model, adapted from the model created by Daly *et al.*[17] A mountain is described by a series of altitudinal zones in sequence; in this work, always five (Fig. 3). Each zone is parameterized with a length and has its own temperature, rate of continuous precipitation and concentrations of contaminant in its compartments.

Each zone contains only two environmental compartments: soil and atmosphere. Zones can differ in their depth of soil, height of atmosphere, and fraction of soil organic matter, but for this work each of these is equal in all zones. Contaminants can move between zones only in the atmosphere. Preferential up-slope wind advects contaminants between zones, as does down-slope mixing, defined as a fraction of the up-slope wind. Wind, and thus contaminants, are free to move out of the model by advecting down from the lowest compartment, or up from the highest compartment.

Unlike the model used by Wegmann *et al.*[16] to explore mountain cold-trapping MountainPOP stands independent of its surroundings: inputs of contaminants to the mountain system are model parameters, not functions of their calculated global fate. Pollutants are emitted only into air of the lowest model zone, representing either transport into that zone from outside of the model domain, or use in the zone where anthropogenic activities such as industry, powered transportation and agriculture are highest.

Chemicals are described wholly by their temperature-dependent partitioning properties and their degradation rates. As this work investigates environmental differences, simulations were run for hypothetical Perfectly Persistent Pollutants (PPPs), which differ only in their K_{OA} and K_{WA}. The temperature dependences of these two coefficients are described by van't Hoff equations in which, for the bulk of the simulations, all PPPs had the same energies of phase transfer (ΔU_{OA} of -83 kJ mol^{-1} and a ΔU_{WA} of -63 kJ mol^{-1}). A small sub-set of simulations was run using ΔU which vary as a function of K_{OA} (see ESI†).

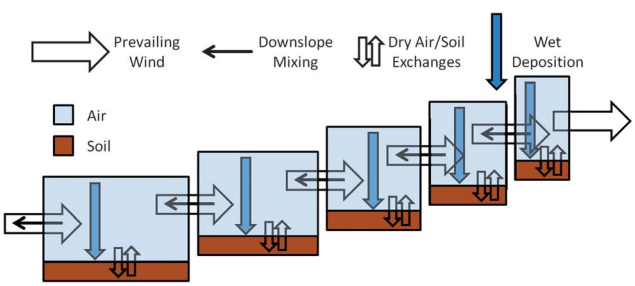

Fig. 3 Conceptual framework for the MountainPOP2.0 model.

Open Access Article. Published on 08 October 2013. Downloaded on 6/2/2026 11:35:24 PM. This article is licensed under a Creative Commons Attribution 3.0 Unported Licence.

Once a PPP is in a zone the processes it undergoes are all functions of these partitioning properties. These processes include: dry- and wet-gaseous exchange between air and soil; partitioning between gas and particle phase in air, and subsequent dry- or wet-deposition to soil for particle-bound species; partitioning between soil organic matter and soil pore air and soil pore water. The temperature dependent equilibrium between environmental phases within each compartment occurs instantaneously, and then the directions and magnitudes of the inter-compartment and inter-zone processes are driven by the instantaneous current concentrations and the advection of the environmental phases themselves, where applicable.

The chief differences between the five zones that allow the model to describe mountains are their temperatures and dimensions.

Mountaintop contamination potential

To compare two chemicals' tendencies to become enriched upslope on a mountain, or any chemical's tendency to become enriched upslope in two different mountains, a Mountaintop Contamination Potential (MCP) was defined as

$$\mathrm{MCP}_i = \frac{\sum_{n=4}^{5} m_{i,\mathrm{Soil}}}{\sum_{n=1}^{5} [m_{i,\mathrm{Soil}} + m_{i,\mathrm{Air}}]} \quad (1)$$

where i is the PPP being modelled, and m_i is mass of i. In words, MCP is the ratio of the mass of PPP i in the soils of the top two zones to the mass of PPP remaining in the entire model domain. Unlike the MCP defined in earlier work with MountainPOP, the mass in air of the top two zones is not included in the numerator.[17] If one considers a PPP that is found almost exclusively in the soil compartment of the model, by this definition a PPP with equal concentrations in all zones would have an MCP of 0.1, because the top two zones contain 10% of the soil in the model, because they are the smallest two zones (see below). That is: MCPs of 0.1 and below are not indicative of cold-trapping.

The scenarios

Four sets of simulations were run: the scale scenarios, in which the length of the model compartments was varied, the precipitation scenarios, the particle scenarios and the temperature scenarios. In each case, the model was run for PPPs with every combination of $\log_{10} K_{\mathrm{OA}}$ from 3 to 12 and $\log_{10} K_{\mathrm{WA}}$ from -3 to 5, in half-log unit increments. It was run for a fixed time of 25 years, yielding MCP_{25}. Some simulations in which the model was allowed to run until near steady-state, giving $\mathrm{MCP}_{\mathrm{SS}}$, appear in the ESI.† Model results are plotted on a CSP defined by $\log_{10} K_{\mathrm{OA}}$ and $\log_{10} K_{\mathrm{WA}}$ with the MCP values represented by colour (Fig. 4, upper left). The partitioning property values in the figures are those for the PPP at 25 °C, not their values in the simulations.

The scale scenarios. An obvious difference between Earth and a mountain is the size. In exploring why the global and mountain models give different results MountainPOP was run at five different scales in which the overall length of the mountain was changed. As the wind-speed is constant this has the effect of altering the residence time in the atmosphere in the model from 40 min at the smallest scale to ~28 days on the largest. 12 km was used to represent a single PEAK; 120 km represented a mountain RANGE; 1200 km served as a scale for a REGION; 12 000 km is roughly the distance from Earth's equator to the Poles and served as a scale for the HEMISPHERE. These scenario names are chosen to give an idea of the size of each mountain as the variable of horizontal scale is explored in isolation, not to suggest the simulation is appropriate for understanding transport on these large scales. The width of the mountains remained the same at 10 km, as did the height of the atmosphere, which at 600 m represents only the boundary layer. The proportions of the lengths of the zones also remained the same. For instance the 12 km long mountain has zones with lengths of 6.2 km, 3.1 km, 1.6 km, 0.77 km and 0.39 km, and the 120 km long mountain has zones with lengths of 62 km, 21 km, 16 km, 7.7 km and 3.9 km. All of the precipitation, particle and temperature simulations presented in the main text were parameterized with the dimensions of the 120 km mountain range.

The precipitation scenarios. In earlier work precipitation scavenging was identified as key in understanding mountain cold-trapping.[18] How much and where rain falls on a mountain may dictate whether or not cold-trapping of a contaminant is observed. Several simulations were run in which the precipitation was varied from the default 1 m of constant annual precipitation in each zone. The NORAIN scenario had 0 m of annual precipitation in every zone. The MORERAIN scenario had 10 m of rain in each zone, and the LESSRAIN scenario only 0.1 m. In the TOPRAIN scenario, annual rainfall was set at 1 m, 0.5 m, 0.2 m, 0 m and 0 m from top to bottom. Finally, in the BOTRAIN scenario the values of the TOPRAIN scenario were reversed.

The particle scenarios. For many chemicals, partitioning to atmospheric particles and subsequent deposition either on their own or with precipitation is an important process for its fate in the environment. To explore the role of this process in mountain cold-trapping, a set of simulations was run in which the Particle Volume Fraction (PVF), the ratio of the volume of particles in the air to the volume of air, was varied. In the LESSPART scenario the PVF was decreased by one order of magnitude from the default value of 10^{-11} and in the MOREPART scenario it was increased by one order of magnitude from the default. In the NOPART scenario the PVF was set to an arbitrarily small number.

The temperature scenarios. Besides the dimensions, the main differences between the five zones in the model are the temperatures. In most simulations the 'lowest' zone has the highest temperature, and each zone is progressively cooler up the mountain. Because the model does not contain any snow, the choice is made to limit the simulations to temperatures above the freezing point of water. So, also staying within the realm of environmental applicability, the maximum temperature range is from 0 °C to 40 °C. Most simulations were run with

 This journal is © The Royal Society of Chemistry 2013

Open Access Article. Published on 08 October 2013. Downloaded on 6/2/2026 11:35:24 PM.
This article is licensed under a Creative Commons Attribution 3.0 Unported Licence.

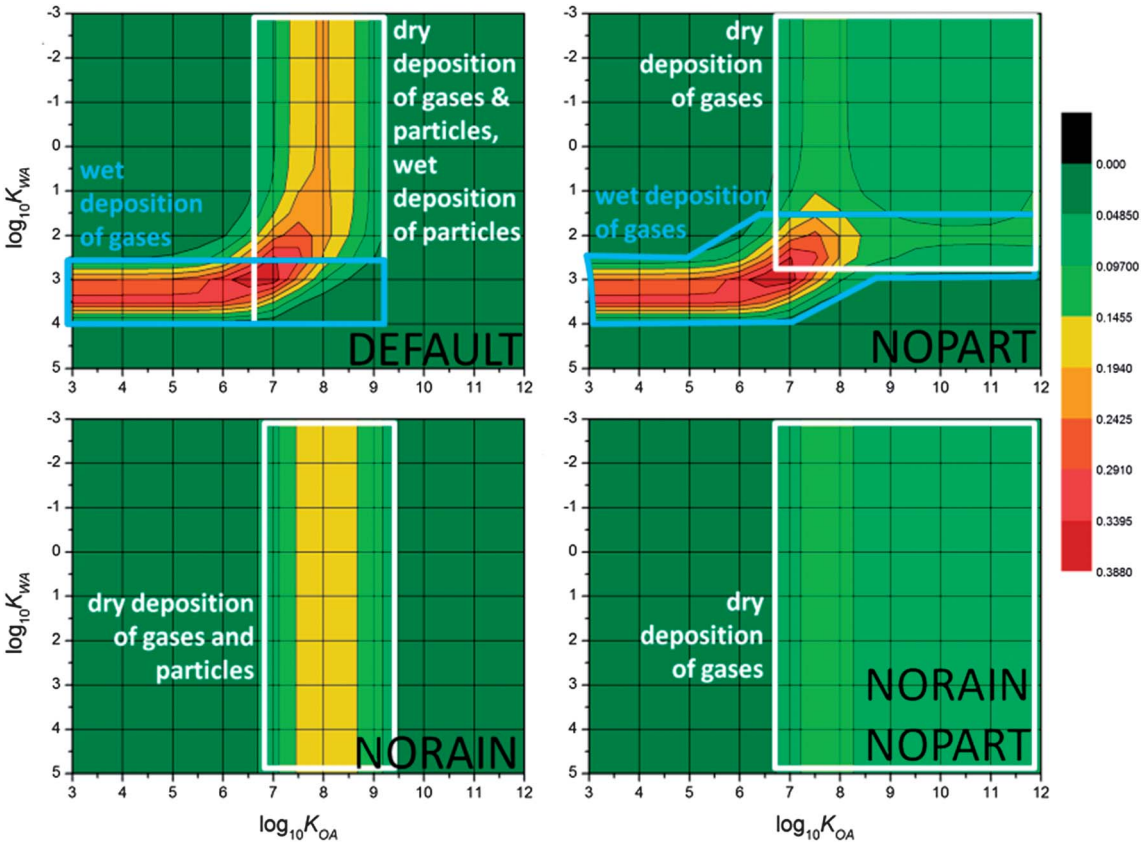

Fig. 4 Chemical space plot of the mountaintop contamination potential MCP_{25} of the default scenario for the 120 km mountain (upper left); that mountain with no atmospheric particles (upper right); that mountain with no rain (lower left); that mountain with neither rain nor atmospheric particles (lower right). Note the scale of $\log_{10} K_{WA}$ has been inverted to place the most volatile PPPs in the upper-left of the CSP.

temperatures of 7 °C, 12 °C, 17 °C, 22 °C and 28 °C. A handful of simulations were run with different temperature scenarios. MAXdT had zones, from top to bottom, with constant temperatures of 0 °C, 10 °C, 20 °C, 30 °C and 40 °C. COLDdT used 0 °C, 5 °C, 10 °C, 15 °C and 20 °C, WARMdT used 10 °C, 15 °C, 20 °C, 25 °C, and 30 °C, and HOTdT used 20 °C, 25 °C, 30 °C, 35 °C and 40 °C. Finally, in NOdT0, NOdT20 and NOdT40 all 5 zones had temperatures of 0 °C, 20 °C and 40 °C, respectively. No simulations in this work included seasonality and none had diurnal temperature changes.

Results and discussion

Interpreting the CSPs

The CSP for the default scenario is shown in Fig. 4, upper left. A band of high MCP perpendicular to the $\log_{10} K_{WA}$ axis (referred to as a 'K_{WA} band' hereafter), evident in the CSP for the default scenario at a $\log_{10} K_{WA}$ of ~3.5 (Fig. 4, upper left), suggests that precipitation plays a role. PPPs that partition more to the air than those along this band (lower K_{WA}, at top of plot) will move through the model domain and exit without being scavenged by precipitation. PPPs that partition too much to water from air (higher K_{WA}, at bottom of plot) will be scavenged as gases in the lower zones of the model and will not be available for precipitation scavenging in the top two zones. PPPs with $\log_{10} K_{WA}$ within that band will undergo wet-gaseous scavenging and be deposited to the soil in the top two zones more than any others. In the default scenario the top two zones are colder than the others. This decrease in temperature increases K_{WA} and therefore scavenging efficiencies. As was argued in earlier work,[18] those that are within the band are those that are not efficiently scavenged by rain at the higher temperatures lower on the mountain but are efficiently scavenged by rain at the lower temperature higher on the mountain (Fig. 2).

The band of high MCP perpendicular to the $\log_{10} K_{OA}$ axis (referred to as a 'K_{OA} band' hereafter), evident in the CSP for the default scenario at a $\log_{10} K_{OA}$ of ~8.0 (Fig. 4, upper left), can be somewhat similarly explained. Octanol is used in the model to calculate partitioning to organic matter,[23] and thus to particles in soils and the atmosphere. PPPs with sufficiently low K_{OA} (left side of the plot) will simply move through the model and exit without appreciably interacting with soil or particles, and thus have low values of MCP. PPPs with sufficiently high K_{OA} (right side of plot) will partition relatively more to soils and particles. Soils are not mobile in MountainPOP, and atmospheric particles are efficiently scavenged by precipitation. Thus these PPPs will remain in the lower zones of the model and not exhibit the strongest up-slope enrichment. PPPs that have K_{OA}s within the band reach the highest zones and are transferred to the soils there by either dry deposition or wet particle deposition. Similar

Open Access Article. Published on 08 October 2013. Downloaded on 6/2/2026 11:35:24 PM.
This article is licensed under a Creative Commons Attribution 3.0 Unported Licence.

to scavenging of gases, this is partly driven by the change in phase equilibrium from air to organic matter caused by the lower temperatures higher on the mountain in the default scenario (Fig. 2).

The two bands of high MCP meet in the lower middle of the CSPs. However, the highest MCPs occur not at the projected intersection of the two bands, but at slightly lower K_{WA} and K_{OA} – that is for generally more volatile PPPs than might be surmised taking the sums of the processes. However, PPPs right at the projected intersection of the bands undergo deposition to surface media by all processes simultaneously, and thus are removed more efficiently from the atmosphere. PPPs thus removed are not available for deposition in the highest two zones, and show reduced MCP compared to the slightly more volatile species. Looked at from the other direction, some PPPs that would leave the mountain without being deposited based only on their K_{WA} or K_{OA} become efficiently deposited in the highest two zones when they are subject to all deposition processes.

Further insight into the various deposition processes leading to cold-trapping can be garnered by 'shutting off' individual routes of deposition. Fig. 4, upper right displays the CSP of the NOPART scenario – *i.e.*, the default scenario with the atmospheric particles removed. This leaves dry-gaseous deposition as the only K_{OA} driven mechanism and gas scavenging as the only K_{WA} driven mechanism for cold-trapping. The results of the NORAIN scenario are displayed in Fig. 4, lower left. Here only dry deposition of gases and particles is possible. The results of removing both rain and particles appear in Fig. 4, lower right, revealing potential cold-trapping driven only by dry gaseous deposition (Fig. 2).

Without particles the K_{OA} band becomes quite wide and extends to high $\log_{10} K_{OA}$ values (Fig. 4), upper right and lower right, suggesting that dry gaseous deposition has a lower specificity than the other processes. Only when particle concentrations are very low does the K_{WA} band extend across the entire chemical space (Fig. 4), upper right, and even then it is shifted to lower K_{WA} by the overlap noted above. Which of the two K_{OA} dependent mechanisms causes the K_{OA} band evident in Fig. 4, upper left? Even though the strongest bands from dry-gaseous-only (Fig. 4), upper right or lower right, and dry-particle-and-dry-gaseous-together (Fig. 4, lower left) are very close, their magnitudes can be compared, which reveals that dry gaseous and dry particle deposition contribute about equally to the high MCP_{25} of PPPs with $\log_{10} K_{OA}$ around 8.

High and low values of MCP within a scenario are of course relative: the PPP with the maximum MCP (MCP_{MAX}) does not necessarily have most of its mass in the highest two zones. In previous work,[18] contamination potentials were normalized to make them easier to compare. Here MCPs are not normalized and this highlights other important differences between mountains. On the 12 km mountain, between 44% and 50% of the masses of the PPPs with the highest MCPs are found in the soils of the top two zones after 25 years. After the same simulation time, less than 0.5% of the PPP with the highest MCP is in the soils of the top two zones of the 12 000 km mountain. Even though this cold trapping potential is higher than that of the other PPPs under the same circumstances the low absolute value suggests that cold trapping is insignificant as it is lower than the threshold of 10% indicating uniform soil concentrations with altitude. In fact, 0.1 is the highest value of MCP assigned in a mountain in which no discernible mechanism of upslope enrichment is present (see Fig. S1†).

Having partially disentangled the different deposition processes (Fig. 2), the temporal scales at which they operate become a question. Fig. 5 compares MCPs for four different deposition regimes as a function of time: wet-gaseous deposition (blue); dry-particle and dry-gaseous deposition (burgundy); dry-gaseous deposition (orange); dry-gaseous deposition in the absence of a temperature gradient (green). Each curve represents the PPP with the highest MCP subject to that regime, but all on the default mountain. It is again clear that, in time, wet-gaseous deposition leads to much greater MCPs than the other processes, followed by combined dry processes, dry-gaseous alone and dry-gaseous with no temperature gradient. The initial rates of increase in MCP are intriguing: the model suggests that for a handful of years, novel contaminants that undergo dry deposition processes will accumulate in soils at high elevations more rapidly than those undergoing wet-gaseous deposition. This at first appears counter-intuitive, as wet deposition ought to occur much more rapidly than dry, but this seeming contradiction is the likely explanation: because of rapid deposition PPPs that are wet scavenged take longer to reach the higher zones in the model. After an initial phase the wet-gaseous line quickly outpaces the dry processes line. This initial phase occurs below the MCP threshold of 0.1 noted above, so while the PPPs are collecting in the soils of the highest two zones, upslope enrichment is not yet occurring. Wet and dry processes are again difficult to separate at this juncture, as they both cross this threshold at the same simulated time. The dry-gaseous processes with and without a temperature gradient both eventually cross the threshold after twice and four-fold the time of the faster processes, respectively.

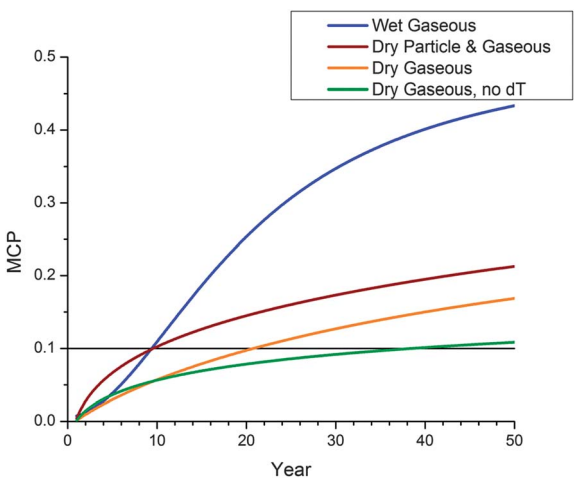

Fig. 5 MCP as defined in EQ1 as a function of time for different deposition regimes: MCP less than 0.1 do not indicate upslope enrichment as this value would be attained by a PPP at the same concentration in the soils of every zone.

 This journal is © The Royal Society of Chemistry 2013

Open Access Article. Published on 08 October 2013. Downloaded on 6/2/2026 11:35:24 PM.
This article is licensed under a Creative Commons Attribution 3.0 Unported Licence.

The role of spatial scale in cold-trapping

Fig. 6 contains chemical space plots of the results from altering the size of the simulated mountain. The names assigned to each scenario give an idea of the scale: they are not meant to suggest that the results represent cold-trapping in, for instance, the entire Northern Hemisphere. The 120 km long RANGE scenario has the greatest MCP values for PPPs with a K_{WA} band at $\log_{10} K_{WA}$ ~3.5 and K_{OA} band at $\log_{10} K_{OA}$ of ~8. MCP_{25} for the larger mountains shows that as the length of the mountain increases the bands of high MCP move to lower values of $\log_{10} K_{WA}$ and $\log_{10} K_{OA}$: the 12 000 km HEMISPHERE mountain has a K_{WA} band at $\log_{10} K_{WA}$ ~2.5 and a K_{OA} band at $\log_{10} K_{OA}$ ~7, but because the maximum MCP_{25} for this enormous mountain is very small compared to the smaller mountains, this is not visible (Fig. 6). These features are apparent when the CSP is scaled to its own maximum (Fig. S3d†).

Increasing the length of the mountains increases a PPP's residence time in the model domain. The velocity of the wind is the same in each of these simulations, so it takes longer for the contaminants to move to the higher zones on the longer mountains. This change in residence time can account in part for the changes in the locations of both the K_{WA} and K_{OA} bands. The PPPs that exhibit the highest MCP on the 12 km mountain partition from the air to water more than those on the increasingly longer mountains: the difference between the smallest and largest mountains is an order of magnitude – that is, 1 log unit. The increased residence time allows more time for wet-gaseous deposition, so every PPP is more likely to be scavenged prior to reaching the highest two zones: that is not to say the shift significantly affects the fate of every PPP, but only those falling within the K_{WA} band. As a result, PPPs being washed out of the gas phase to the soil in the highest two zones of the largest mountain are those that partition slightly less to water than air than those on the smallest mountain. The shift of the K_{OA} bands to lower values as the size of the mountains increase is similarly explained and also moves about 1 log unit from the PEAK scenario to the HEMISPHERE scenario.

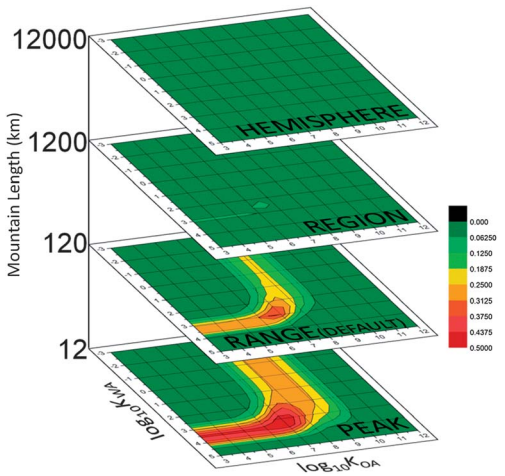

Fig. 6 MCP_{25} as a function of scale, with all CSPs recolored to the MCP_{max} in this figure of 0.5: the vertical scale is the mountain length in km.

That, when allowed to run for longer periods, the K_{WA} and K_{OA} bands of the longer mountains approach the values found on the smaller mountains also points to residence time as the driver behind the observed differences in MCP_{25}. For real contaminants on real mountains, this suggests that for some species, whether or not it is found to exhibit upslope enrichment in part depends on the length of time it has been emitted to the environment.

The role of precipitation in mountain cold-trapping

The simulations involving scale suggested that precipitation is an extremely important process in determining which PPPs exhibit the highest MCPs, and this is bolstered by examining the results of the precipitation scenarios. Fig. 7 displays the CSPs for all of the precipitation scenarios. The DEFAULT scenario, recoloured to the MCP_{MAX} for the whole figure, appears for reference. In the extreme case of NORAIN there is no K_{WA} band at all, and the broad log K_{OA} band is centred somewhere between 8 and 8.5. Without rain to wash contaminants from the atmosphere to the soil the preference of a PPP for water or gas phases becomes irrelevant. Soil moisture in these simulations was not a function of the rate of precipitation, and was set at a constant. In the NORAIN scenario it had to be set quite low to prevent relatively hydrophilic PPPs from partitioning strongly to the moisture in the soil compartment. Please see the ESI† for further information about the treatment of soil water and its impact on this scenario.

While the K_{OA} band for the LESSRAIN scenario remains similar to the band from NORAIN, it is at a higher K_{OA} value than in the default scenario and much higher than in the MORERAIN scenario. Clearly there is a threshold below which rain is too scarce to scavenge particles efficiently enough to be more important than dry deposition processes. The K_{WA} band in MORERAIN is shifted towards the gas-phase and in LESSRAIN towards the water phase compared to the default. It appears that increased rain volume means PPPs that have a greater preference for the gas phase with respect to both water and particles exhibit mountain cold-trapping.

The BOTRAIN scenario results (Fig. 7, lower right) have no K_{WA} band: under these conditions no rain occurs in the highest two zones, so there is no wet contribution to high MCP. Upslope enrichment occurs only for PPPs that undergo dry gaseous and particle bound deposition which occurs at the same $\log_{10} K_{OA}$ as in the NORAIN scenario. There is still a threshold of K_{WA} below which PPPs are washed out in lower zones, so precipitation still plays a role in determining MCP, unlike in the NORAIN scenario.

Fig. 7, upper right is the CSP for the TOPRAIN scenario: it stands out from the others with an MCP_{MAX} double that of any other scenario. The highest MCP is for PPPs with a $\log_{10} K_{WA}$ of around 3.5. In contrast, the same size mountain with no gradient in the precipitation rate (Fig. 7, left) has an MCP_{MAX} where the two bands overlap at $\log_{10} K_{WA}$ of 3. This bolsters the assertion above that the upper limit on K_{WA} to give high MCP is caused by PPPs being washed out in the lower zones of the mountain. When the rain is small or nil in the lower compartments a wider range of PPPs with higher K_{WA} arrive in the higher zones and are deposited to soils by the ample precipitation there.

Open Access Article. Published on 08 October 2013. Downloaded on 6/2/2026 11:35:24 PM.
This article is licensed under a Creative Commons Attribution 3.0 Unported Licence.

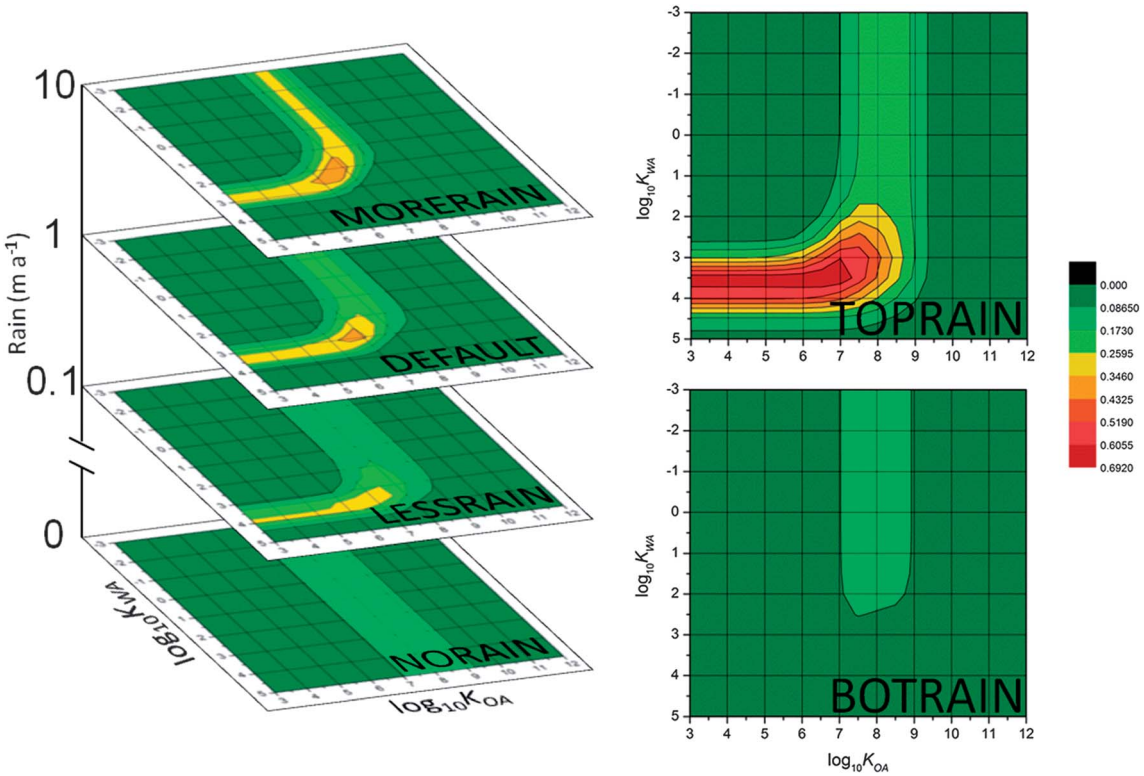

Fig. 7 MCP_{25} as a function of precipitation: the 4 scenarios with the same amount of precipitation in each zone are NORAIN (0 m a^{-1}), LESSRAIN (0.1 m a^{-1}), the default (1 m a^{-1}) and MORERAIN (10 m a^{-1}); the TOPRAIN scenario and the BOTRAIN scenario have precipitation gradients; all CSPs are recolored to the MCP_{MAX} of 0.7 in this figure.

Another feature of TOPRAIN is that the K_{OA} band has lower MCPs than the K_{WA} band – in fact MCPs in this band are no higher than the default. It still exists, meaning there is still a balance between not getting to the highest zones and not being trapped in the model domain based on partitioning to soil or particles, but it is relatively less important to high MCP than gaseous precipitation scavenging in the higher zones. In other words, there is an upper limit to the effect of precipitation scavenging on particle bound contaminants, most likely because the concentration of particles in air is finite.

One aspect of precipitation not explored here is the effect of its intermittent nature.[24,25] The issue was deemed too complex for the scope of this study, because it would require the consideration of lengths and intensity of precipitation events, the lengths of the intervals between such events, and the relative temporal arrangement of the precipitation events at different altitudes. Because wet precipitation has a role to play in both mitigating and enhancing mountain cold-trapping, we suspect that scenarios with intermittent precipitation would lead both to higher and lower MCP than scenarios with the continuous rain assumption.

The role of atmospheric particle concentration in mountain cold-trapping

Altering the precipitation scenarios revealed that dry deposition is very important for PPPs whose MCP_{MAX} are dictated by their K_{OA} values. This is somewhat surprising, given the effectiveness of scavenging of particles by precipitation, but the above scenarios also revealed a limit to the efficiency of wet-particle-bound cold-trapping, perhaps because of a dearth of particles in the atmosphere: the actual mass of contaminant sorbed to particles depends strongly on the concentration of particles available for sorption.

CSPs from the MOREPART and the LESSPART scenarios are shown in Fig. 8, along with the default and NOPART scenarios, all recoloured to MCP_{MAX} for the entire figure. The default mountain results and the LESSPART results are largely similar in that MCP_{MAX} for both occurs at $\log_{10} K_{WA} \sim 3.5$. The K_{OA} band at $\log_{10} K_{OA} \sim 8$ seen in the default is less strong, much broader and centred around $\log_{10} K_{OA} \sim 8.5$ in the LESSPART scenario. The reduced availability of particles to which to sorb reduces the mass of these PPPs deposited to the soils of the highest two zones, and thus their MCPs, but does not markedly change their identities: the band is slightly broader towards the organic matter side, however, showing once again that a decrease in the available phase causes a shift of the corresponding band of MCP towards that phase.

The most striking feature of the MOREPART scenario is that the K_{OA} band shows very high MCP values, which is not seen in any other scenario with uniform rain in all zones. The increased availability of particles causes greater masses of semi-volatile PPPs to be sorbed and thus deposited, increasing the importance of particle-bound relative to wet-gaseous deposition. The

 This journal is © The Royal Society of Chemistry 2013

Open Access Article. Published on 08 October 2013. Downloaded on 6/2/2026 11:35:24 PM.
This article is licensed under a Creative Commons Attribution 3.0 Unported Licence.

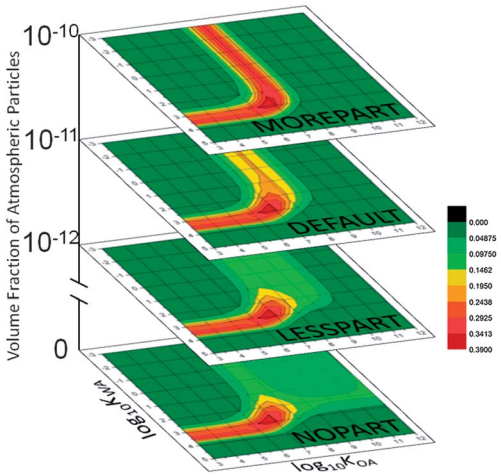

Fig. 8 MCP_{25} as a function of the amount of organic particles in the atmosphere, all recoloured to the MCP_{MAX} of 0.4 in this figure; the NOPART scenario, LESSPART, default and MOREPART had no particles, volume fractions of atmospheric particles of 0, 10^{-12}, 10^{-11} and 10^{-10}, respectively.

K_{OA} band is also centred on $\log_{10} K_{OA}$ ~7.5, a half-log unit lower than the default mountain. As well, the increased particle concentration causes an increase in the amount of a PPP with a slightly higher K_{OA} that will be removed from the atmosphere to the soil before reaching the highest two zones, and decreases the amount of a PPP with a slightly lower K_{OA} that will be deposited in those two highest zones.

That the PVF has such a clear influence on MCP acts as evidence that, under these conditions, sorption to particles and their subsequent deposition is a more important process than dry-gaseous deposition to soil in driving upslope enrichment of contaminants in surface media. This stems, in part, from dry-gaseous deposition occurring only at the air/soil interface, while sorption to particles and their scavenging by precipitation both occur throughout the entire volume of the atmosphere. A note about the relative importance of dry- and wet-particle-bound deposition appears in the ESI.†

The role of temperature in mountain cold-trapping

The phrase 'cold-trapping' indicates that temperature is a key driver in causing contaminants to undergo upslope enrichment. More precisely, the phrase suggests that a gradient in temperature from the bottom to the top is a requirement for a mountain to exhibit upslope enrichment of a contaminant. The effect of the steepness and range of this temperature gradient on MCP was explored using a set of scenarios in MountainPOP. CSPs of the results from these calculations are in Fig. 9.

As with the CSPs from the other scenario sets, all show the familiar K_{WA} and K_{OA} bands. However, from the COLDdT to the WARMdT to the HOTdT (Fig. 9, left) there is a change in the location of these bands of about one half log unit away from the air phase to the condensed phases, water and organic matter. That is, the balance point between a PPP partitioning so much to the gas phase that it moves through the model without being deposited and partitioning so much to the condensed phases that it does not travel up the mountain changes with the temperature. Recall, however, that the axes display the equilibrium partitioning coefficients of each PPP at 25 °C, not at the model temperature: the transitions from air to water or air to soil or particles are occurring at the same K_{WA}s and K_{OA}s, respectively, but at different points in each virtual mountain. Thus, in colder scenarios more volatile PPPs have high MCPs than on warmer mountains, and *vice versa*.

Fig. 9, middle is the CSP for the MAXdT scenario. It has bands of high MCP at $\log_{10} K_{WA}$ ~3.5 and $\log_{10} K_{OA}$ ~8. In that regard it is similar to the CSP for the WARMdT scenario. The magnitudes of MCP between the two are quite different, however: the MCP_{max} for the WARMdT scenario is 0.46, while that for the MAXdT scenario is 0.83. In the extreme scenarios where the temperature gradient is removed altogether this pattern is reinforced: the NOdT0 scenario assigns relatively high MCP to more volatile PPPs than any other temperature scenario, while the NOdT40 scenario assigns relatively high MCP to less volatile PPPs (Fig. 9, right). The NOdT20 scenario assigns its highest MCPs to a very similar set of PPPs to those scenarios that have the same mean mountain temperature, MAXdT and WARMdT. However, the absolute MCP_{MAX} values for the NOdT scenarios are very low, and always less than 0.07. This is below the 0.1 threshold that indicates equal concentrations in the soils of all zones.

Overall, the temperature simulations limited to 25 years reveal two things: the identities of the PPPs assigned high MCPs depend strongly on the mean temperature of a mountain; the magnitudes of the MCP assigned to those PPPs depend strongly on the slope of the temperature gradient, and without a gradient upslope enrichment does not occur. A brief discussion on the effect of a temperature gradient on the global scale appears in the ESI.†

On the differences between mountain and polar cold-trapping

That scale alone cannot account for all the difference predicted between mountain and polar cold-trapping indicates additional factors must contribute to the lower volatility of PPPs undergoing mountain cold-trapping compared to those undergoing polar cold-trapping. One clear difference between the models is that the top of the mountain is open and allows contaminants to move out of the modelled domain, while on the global scale contaminants that leave the highest latitudes cycle back to lower, warmer latitudes where they are less likely to deposit, and then can move back again to the higher latitudes. This would mean that higher volatility species are more likely to collect in the highest latitudes than those that collect in the highest mountain elevations.

The precipitation scenarios offer little in the way of explaining the model differences. The globe is somewhat like the BOTRAIN scenario, as precipitation rates decrease from the mid-latitudes to the poles. However, while the strength of cold-trapping is expected to be different, the identities of the cold-trapped species on the K_{OA} band remain the same. Furthermore, model simulations of the Arctic show the highest contamination potentials along a K_{WA} band, which does not match the BOTRAIN scenario, which sits at an extreme with zero precipitation in the highest zones.

Open Access Article. Published on 08 October 2013. Downloaded on 6/2/2026 11:35:24 PM.
This article is licensed under a Creative Commons Attribution 3.0 Unported Licence.

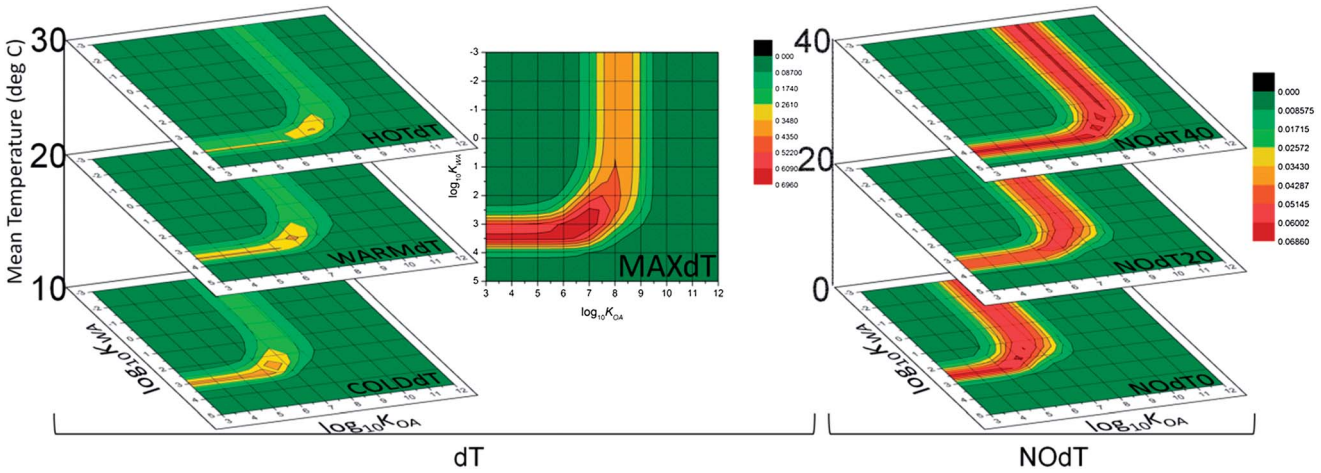

Fig. 9 CSPs of MCP_{25} from the temperature scenarios: the COLDdT, WARMdT and HOTdT scenarios each span 20 °C centred at 10 °C, 20 °C and 30 °C respectively, while the MAXdT scenario spans 40 °C centred at 20 °C, and all are recoloured to MCP_{MAX} for the dT results; the NOdT0, NOdT20 and NOdT40 scenarios had 0 °C, 20 °C AND 40 °C, respectively, in all five zones of the mountain and are recoloured to the MCP_{MAX} from the NOdT results.

In contrast to individual mountains, the atmospheric particle concentration on the global scale may vary substantially. This may explain part of the difference in the results when modelling mountain *versus* polar cold-trapping. The global scale model contains fewer particles in the polar atmospheres than at lower latitudes: as we see here where fewer particles are available dry-gaseous deposition becomes more important than dry particle-bound deposition, which favours deposition of more volatile species, specifically along the K_{OA} axis. As MountainPOP is not configured to accept different concentrations of atmospheric particles in different zones, this was not explored further.

Overall, the differences between mountain and polar cold-trapping appear to be a complex combination of all of the factors manipulated here, and perhaps others. The following conjecture may be considered, where low refers to the bottom of the mountain and low latitudes, and top the mountaintop and Earth's poles: the much longer travel distance at the global scale dictates species must be generally more volatile to reach the top without being removed; lower particle concentrations at the top of the Globe cause both dry- and wet-gaseous deposition to be greater drivers of cold-trapping, simultaneously shifting the K_{OA} band to more volatile species while increasing the relative MCP of the K_{WA} band, despite the lower precipitation; species that are deposited but revolatilize at the Globe's top are likely to re-circulate and redeposit at the Globe's top, again cold-trapping more volatile species in the global model than the mountain model, from which they are free to depart.

Implications for identifying mountain cold-trapping in the field

The present work examines only virtual mountains to elucidate potential mechanisms of mountain col-trapping and the factors that control them. No seasonality is included, precipitation occurs at a constant rate and there is no snow compartment in the model. Furthermore, the investigated hypothetical chemicals do not degrade and only enter the system at the lowest elevation. Despite this lack of reality, these results can aid in the interpretation of field measurements in which samples are collected along an elevational transect and analyzed for organic pollutants.

The model reveals that the key environmental factors that lead to strong mountain cold-trapping are a high atmospheric organic particle load, a strong gradient of precipitation that increases upslope, and a large temperature gradient from the valley to the mountaintop. The first is illuminated in the MOREPART scenario which increases the magnitude of the K_{OA} band, the second in the TOPRAIN scenario which gives greater magnitude to the K_{WA} band and the third in the MAXdT scenario which increases the magnitude of both the K_{OA} and the K_{WA} bands. This suggests that the optimal conditions for cold-trapping should exist where all three of these conditions are present. Here a detail not captured within the model is revealed: the volume fraction of particles is not affected by precipitation (this is necessary because rain is not modelled as episodic, but it rains a little bit all of the time). In reality, on a mountain where rain falls low on the mountain the atmospheric particles are quite readily washed from the air and are thus not available to sorb contaminants higher on the mountain. On a mountain where rain falls only at the higher elevations, as in the TOPRAIN scenario, this low elevation washout would not occur and this relatively higher concentration of available particles for sorption would cause an increase in the relative magnitude of mountain cold-trapping. The Northern slopes of the European Alps make good candidates for real mountains on which precipitation falls more at the top than the foot of the mountains. This is because the air arriving from the North is likely not too close to 100% relative humidity. This means that it can undergo a certain amount of orographic uplift, and hence cooling, without reaching saturation, and forming clouds and precipitation. Furthermore, before reaching the foot of the Alps the air passes over areas of high population density and industry, where anthropogenic emissions of organic particles

 This journal is © The Royal Society of Chemistry 2013

Open Access Article. Published on 08 October 2013. Downloaded on 6/2/2026 11:35:24 PM.
This article is licensed under a Creative Commons Attribution 3.0 Unported Licence.

are quite high, and over densely forested areas and areas of intense agriculture, where natural organic substances are emitted which can undergo processing into larger secondary organic particles capable of sorbing SVOCs. Additionally, the great height of the European Alps causes a large temperature difference between the bases and the summits. All together, these ought to lead to strong mountain cold-trapping of SVOCs that lie along both the K_{WA} and the K_{OA} bands.

The air arriving at the Southern slope of the Himalayas during monsoon season also arrives with a high concentration of atmospheric particles. Annual background concentrations of inhalable particles in the area hover around 50 μg m^{-3}, comparable to concentrations in urban areas in the West.[26] These air masses are famously laden with vast quantities of water vapour as well, having earlier origins over the oceans, yet often arrive at the base of the mountains without raining out the water or the particles. Upon meeting the foothills, the air undergoes orographic uplift, and undergoes cooling, leading to the torrential monsoon rains of the Khasi Hills. It generally rains less further upslope, which should mean the magnitude of cold-trapping would be less than in the European Alps, and if the bulk of the particles are indeed washed out low on the mountain, SVOCs associated with the K_{OA} band would not likely reach higher elevations.

In general, one can expect to find that different contaminants are undergoing cold-trapping in different mountains. In particular, mountains with different mean temperatures will sequester different pollutants at high elevations. Where in the mountain system precipitation occurs will also affect which pollutants are found at high elevations. And precipitation together with the magnitude of the temperature difference between the bottom and the top of the mountain will dictate whether or not cold-trapping is observed at all: without sufficient deposition differences, concentration differences between sites driven by cold-trapping will be smaller than the variability caused by other factors.

No real chemicals are modelled in this work: PPPs do not degrade by any means, but simply cycle until leaving the model domain. However, one can get an idea of what real chemicals may exhibit mountain cold-trapping by locating them in the chemical space by their partitioning properties at 25 °C. Fig. 10 displays a few example groups of chemicals overlain on the results from the DEFAULT Scenario. Sufficiently persistent chemicals that overlap areas of high MCP are theorized to be found at greater concentrations high on mountain slopes than near the bottoms of mountains.

The polychlorinated biphenyls (PCBs) span a wide range of partitioning properties (Fig. 10, dark blue). Were these overlain on the CSPs from the different temperature scenarios it would suggest that different congeners will be cold-trapped on different mountains. Warm, tropical mountains, such as the mountains of Costa Rica or Brazil, are predicted to cold-trap tetra- and penta-chlorinated PCBs (*e.g.* PCB52, PCB101), while cold high-latitude mountains, such as those of the Alaskan Brooks Range or Western Scandinavia, are predicted to trap lighter mono-, di- and tri-chlorinated PCBs (*e.g.* PCB3, PCB8, PCB15).

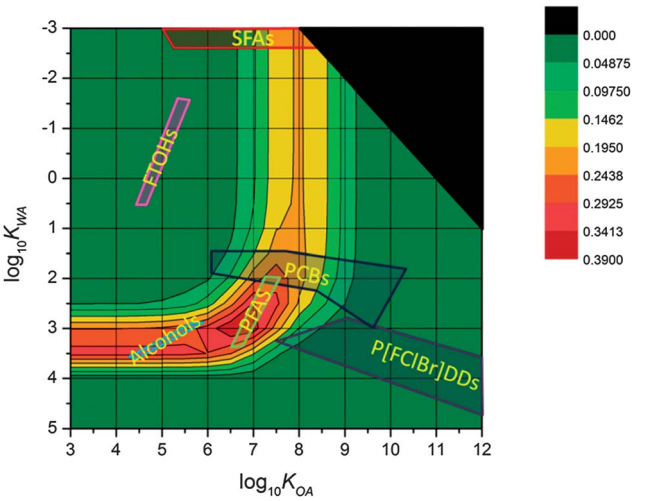

Fig. 10 Real chemicals in the CSP overlain on the results of the DEFAULT scenario: the fluorotelomer alcohols (FTOHs, in pink, data from ref. 27) tend to reside in the atmosphere and are not predicted to exhibit mountain cold trapping; poly-halogenated dibenzo-*p*-dioxins (P[FClBr]DDs, in purple, from ref. 31) favour organic matter strongly and are not predicted to be cold-trapped; small semifluorinated alkanes (SFAs, in red, from ref. 32) are quite volatile but also partition to organic matter and may undergo mountain cold-trapping; the polychlorinated biphenyls (PCBs, in dark blue[30]) span a wide range of partitioning properties, and those of intermediate properties are expected to undergo mountain cold-trapping on the DEFAULT mountain; perfluoroalkylsulfonamides (PFAS, in bright green, from ref. 27) are expected to undergo strong mountain cold-trapping; were simple, non-water-miscible alcohols (in light blue, from ref. 29) persistent, they would also exhibit mountain cold-trapping; the black triangle masks the area where log K_{OW} is greater than 11, where no organic chemicals fall.[33]

At the very top of Fig. 10 are some semi-fluorinated alkanes (SFAs, in red), although most of these appear at K_{WA} values that are lower than those in the figure. Imagining this band on the CSPs of the particle scenarios suggests that without sufficient particles in the air, the SFAs will not exhibit mountain cold-trapping, but will be cold-trapped where particles are plentiful. It follows that one might expect to find SFAs cold-trapped on the highly urbanized mountains North of Vancouver, but not on Mount Erebus in Antarctica.

The model predicts that the family of perfluoroalkylsulfonamides (PFASs, in light green), precursors to perfluorosulfonates,[27,28] may exhibit strong mountain cold-trapping as they fall directly in the area of overlapping bands of the DEFAULT Scenario. Placed on the CSPs from the particle scenarios the positions of the PFASs would suggest that the amount and nature of available atmospheric particles would have little impact on their cold-trapping. However, overlaying them over the precipitation or temperature CSPs hints that on a mountain that was too dry or too warm the PFASs would undergo much less upslope enrichment than on the DEFAULT mountain. PFASs fall in the zone in which the TOPRAIN scenario predicts the strongest mountain cold-trapping. Some of the Spring Mountains of Nevada are wetter on the top than the bottom. Surrounded by desert, air on these mountains must undergo significant uplift before cooling to the dew point and thus precipitation is greater higher on the mountains than at their bases, thus PFASs may be found to undergo very strong

Open Access Article. Published on 08 October 2013. Downloaded on 6/2/2026 11:35:24 PM.
This article is licensed under a Creative Commons Attribution 3.0 Unported Licence.

mountain cold-trapping there. At the other extreme are some Southern sections of the Andes Mountains: with no precipitation to bring contaminants to the surface high in the mountains, and with bountiful rain on the coastal mountains below to washout contaminants, levels of all organic contaminants are expected to be the same or lower on these mountaintops than in the surrounding area.

Beyond degradation, an additional confounding factor is the history of the pollutant itself, including at what stage it is in its production life-cycle when measured: here, PPPs are released at a constant rate for an unlimited time, while actual pollutants are not. The typical pesticidal POP, for instance, is emitted at low rates upon introduction and at increasing rates as it becomes more widely used, with emissions peaking at the point that phase-out begins and eventually falling to zero when completely banned. As primary emissions drop previous sinks become secondary sources of some pollutants. An animation of MCP as a function of time for PPPs with a 50 years, sinusoidal emissions curve and 100 additional years without emissions can be found at http://www.utsc.utoronto.ca/~westgate/MCPinTime.gif. It is apparent that a wide range of PPPs exhibit mountain cold-trapping at different stages of this progression, although absolute concentrations in the latter third of the simulation are quite low.

Acknowledgements

The authors acknowledge useful comments by James M. Armitage and funding from the Ontario Graduate Scholarship program, and the Natural Science and Engineering Research Council of Canada.

References

1 UNEP Interim Secretariat for the Stockholm Convention, accessed 17/07/2012.
2 F. Wania and D. Mackay, *Ambio*, 1993, **22**, 10–18.
3 T. F. Bidleman, L. M. Jantunen, R. L. Falconer, L. A. Barrie and P. Fellin, *Geophys. Res. Lett.*, 1995, **22**, 219–222.
4 F. Wania and D. Mackay, *Environ. Sci. Technol.*, 1996, **30**, 390A–396A.
5 D. Calamari, P. Tremolada, A. Di Guardo and M. Vighi, *Environ. Sci. Technol.*, 1994, **28**, 429–434.
6 D. Calamari, E. Bacci, S. Focardi, C. Gaggi, M. Morosini and M. Vighi, *Environ. Sci. Technol.*, 1991, **25**, 1489–1495.
7 G. L. Daly and F. Wania, *Environ. Sci. Technol.*, 2005, **39**, 385–398.
8 P. Wang, Q. Zhang, Y. Wang, T. Wang, X. Li, Y. Li, L. Ding and G. Jiang, *Chemosphere*, 2009, **76**, 1498–1504.
9 M. Kirchner, T. Faus-Kessler, G. Jakobi, W. Levy, B. Henkelmann, S. Bernhöft, J. Kotalik, A. Zsolnay, R. Bassan, C. Belis, N. Kräuchi, W. Moche, P. Simoncic, M. Uhl, P. Weiss and K.-W. Schramm, *Environ. Pollut.*, 2009, **157**, 3238–3247.
10 C. Liu, G.-L. Yuan, Z.-F. Yang, T. Yu, X.-Q. Xia, Q.-Y. Hou and L. Chen, *Environ. Earth Sci.*, 2010, **62**, 953–960.
11 M. A. Mast, D. A. Alvarez and S. D. Zaugg, *Environ. Toxicol. Chem.*, 2012, **31**, 524–533.
12 X. Zheng, X. Liu, G. Jiang, Y. Wang, Q. Zhang, Y. Cai and Z. Cong, *Environ. Pollut.*, 2012, **161**, 101–106.
13 M. Bartrons, J. O. Grimalt and J. Catalan, *Limnetica*, 2012, **31**, 155–164.
14 M. Scheringer, F. Wegmann, K. Fenner and K. Hungerbühler, *Environ. Sci. Technol.*, 2000, **34**, 1842–1850.
15 T. Meyer and F. Wania, *Atmos. Environ.*, 2007, **41**, 2757–2767.
16 F. Wegmann, M. Scheringer and K. Hungerbühler, *Ecotoxicol. Environ. Saf.*, 2006, **63**, 42–51.
17 G. L. Daly, Y. D. Lei, C. Teixeira, D. C. G. Muir, L. E. Castillo and F. Wania, *Environ. Sci. Technol.*, 2007, **41**, 1118–1123.
18 F. Wania and J. N. Westgate, *Environ. Sci. Technol.*, 2008, **42**, 9092–9098.
19 G. L. Daly, Y. D. Lei, C. Teixeira, D. C. G. Muir, L. E. Castillo, L. M. M. Jantunen and F. Wania, *Environ. Sci. Technol.*, 2007, **41**, 1124–1130.
20 J. G. Cole and D. Mackay, *Environ. Toxicol. Chem.*, 2000, **19**, 265–270.
21 T. Meyer, F. Wania and K. Breivik, *Environ. Sci. Technol.*, 2005, **39**, 3186–3196.
22 Y. D. Lei and F. Wania, *Atmos. Environ.*, 2004, **38**, 3557–3571.
23 R. Seth, D. Mackay and J. Muncke, *Environ. Sci. Technol.*, 1999, **33**, 2390–2394.
24 E. G. Hertwich, *Environ. Sci. Technol.*, 2001, **35**, 936–940.
25 O. Jolliet and M. Hauschild, *Environ. Sci. Technol.*, 2005, **39**, 4513–4522.
26 D. Giri, K. Murthy and P. R. Adhikary, *Int. J. Environ. Res.*, 2008, **2**, 49–60.
27 H. P. H. Arp, C. Niederer and K.-U. Goss, *Environ. Sci. Technol.*, 2006, **40**, 7298–7304.
28 J. W. Martin, B. J. Asher, S. Beesoon, J. P. Benskin and M. S. Ross, *J. Environ. Monit.*, 2010, **12**, 1979–2004.
29 D. Mackay, W. Shiu, K. Ma and S.-C. Lee, *Handbook of Physical-Chemical Properties and Environmental Fate for Organic Chemicals Volume III: Oxygen Containing Compounds*, CRC Taylor & Francis, New York, 2006.
30 A. Beyer, F. Wania, T. Gouin, D. Mackay and M. Matthies, *Environ. Toxicol. Chem.*, 2002, **21**, 941–953.
31 A. Gawor and F. Wania, *Environ. Sci.: Processes Impacts*, 2013, **15**, 1671–1684.
32 M. M. Plassmann, T. Meyer, Y. D. Lei, F. Wania, M. S. McLachlan and U. Berger, *Environ. Sci. Technol.*, 2010, **44**, 6692–6697.
33 T. N. Brown and F. Wania, *Environ. Sci. Technol.*, 2009, **43**, 6676–6683.

 This journal is © The Royal Society of Chemistry 2013